Mars Science Laboratory CHIMRA: A Device for Processing Powdered Martian Samples

Daniel Sunshine*

Abstract

The CHIMRA is an extraterrestrial sample acquisition and processing device for the Mars Science Laboratory that emphasizes robustness and adaptability through design configuration. This work reviews the guidelines utilized to invent the initial CHIMRA and the strategy employed in advancing the design; these principles will be discussed in relation to both the final CHIMRA design and similar future devices. The computational synthesis necessary to mature a boxed-in impact-generating mechanism will be presented alongside a detailed mechanism description. Results from the development testing required to advance the design for a highly-loaded, long-life and high-speed bearing application will be presented. Lessons learned during the assembly and testing of this subsystem as well as results and lessons from the sample-handling development test program will be reviewed.

Introduction

The CHIMRA (Collection and Handling for *In situ* Martian Rock Analysis) is the sample processing device for the Mars Science Laboratory (MSL). Scheduled to launch in the fall of 2011, MSL is the next step in NASA's search for evidence to determine if the red planet's environment was, or still is, suitable for microbial life. To accomplish this goal, MSL houses an advanced suite of scientific instruments that will be able to ascertain whether the local geological environment contains the chemical building blocks of life. In order to feed science samples directly to these instruments, MSL required a state-of-the-art Sample Acquisition / Sample Processing and Handling (SA/SPaH) subsystem able to collect, sort, and deliver acquired samples to instruments in the rover. Utilizing a five degree-of-freedom robotic arm (Figure 1) and a rotary percussive drill that forms the backbone of a five instrument turret (Figure 2) the SA/SPaH subsystem is able to collect powered rock from depths up to 50 millimeters. This powdered rock is then transferred to the CHIMRA (Figure 3) for processing.

Each of the requirements for an extraterrestrial sample processing device are individually simple, however when combined together, they form a collection of interconnected and dual-purposed device constraints. The sample processing device must both acquire scooped regolith as well as accommodate sample transfer from the drill. The collected regolith or drilled powder must be sorted and separated into either sub-1 millimeter or sub-150 micron particle sizes, reduced to a portion size of 45-65 cubic millimeters for sub-150 micron sample or 45-130 cubic millimeters for sub-1 millimeter sample and delivered to the science instruments on the rover. In addition to these science-driven sampling requirements, a number of self-imposed design constraints were created that are essential to any extraterrestrial sample processing device. These additional design constraints increase the robustness and adaptability of a remotely operated sample processing system. The response to these multi-faceted constraints is an innovative and functionally dense device: the CHIMRA.

* Jet Propulsion Laboratory, California Institute of Technology, Pasadena, CA

Proceedings of the 40th Aerospace Mechanisms Symposium, NASA Kennedy Space Center, May 12-14, 2010

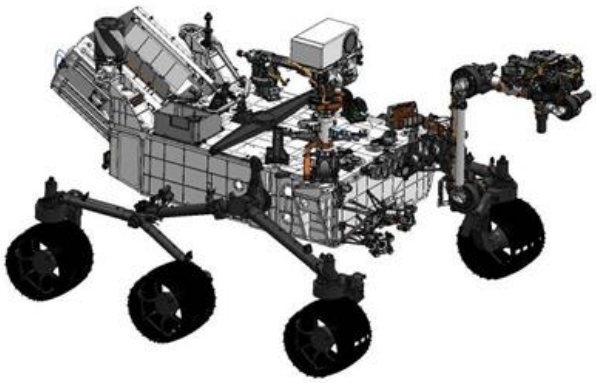

Figure 1. SA/SPaH is a rover-mounted sampling system

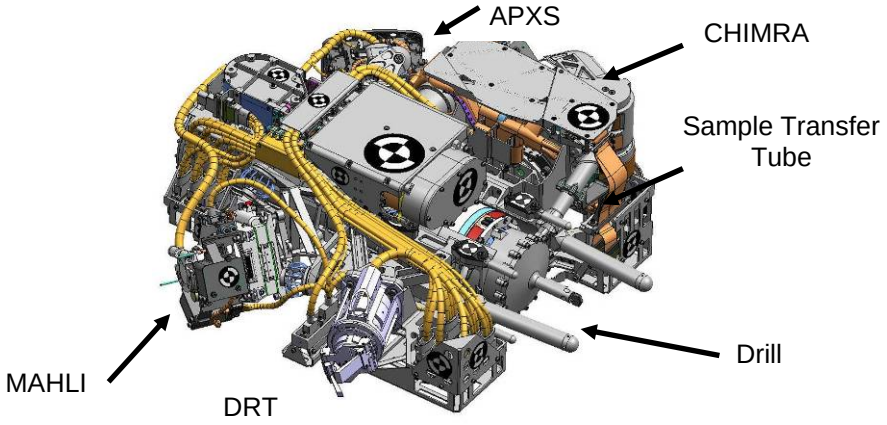

Figure 2. CHIMRA is one of five instruments on the turret

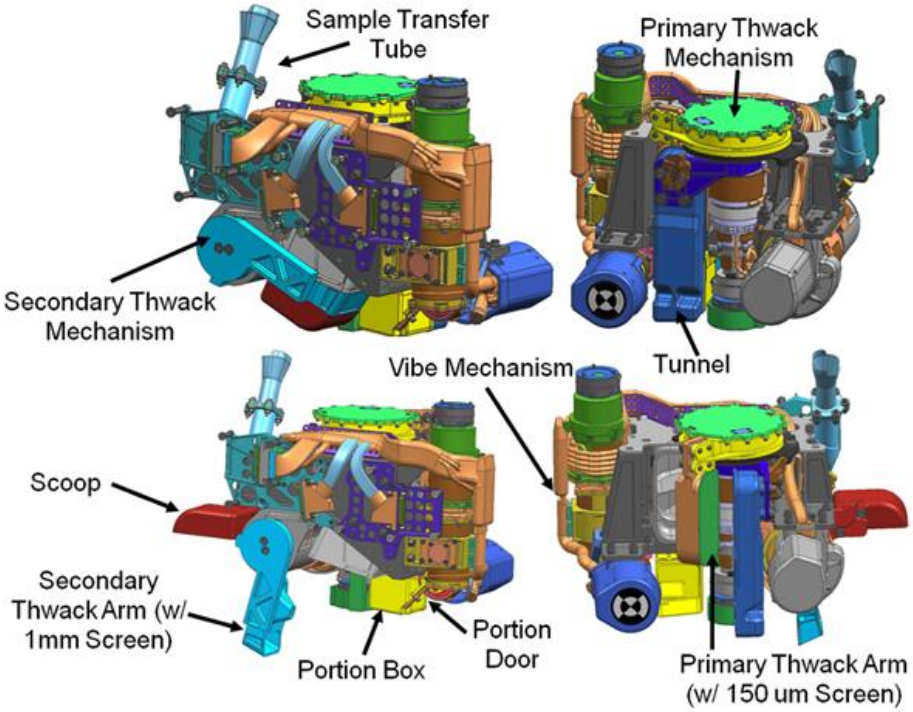

Figure 3. CHIMRA: open and closed configurations

Overview of CHIMRA

The majority of CHIMRA's sample processing functionality is accomplished inherently with the overall design configuration. The internal structure is a labyrinth (Figure 5) that contains two primary passageways used to flow sample into a central processing reservoir from two independent sources: bulk regolith, scooped from the Martian soil by CHIMRA, or powdered sample collected by the drill and transferred via the sample transfer tube. From the central processing reservoir, sample can be diverted through either a 150-micron sieve or a 1-millimeter sieve into two independent portioning chambers. A schematic of the CHIMRA sample processing paths is shown in Figure 4.

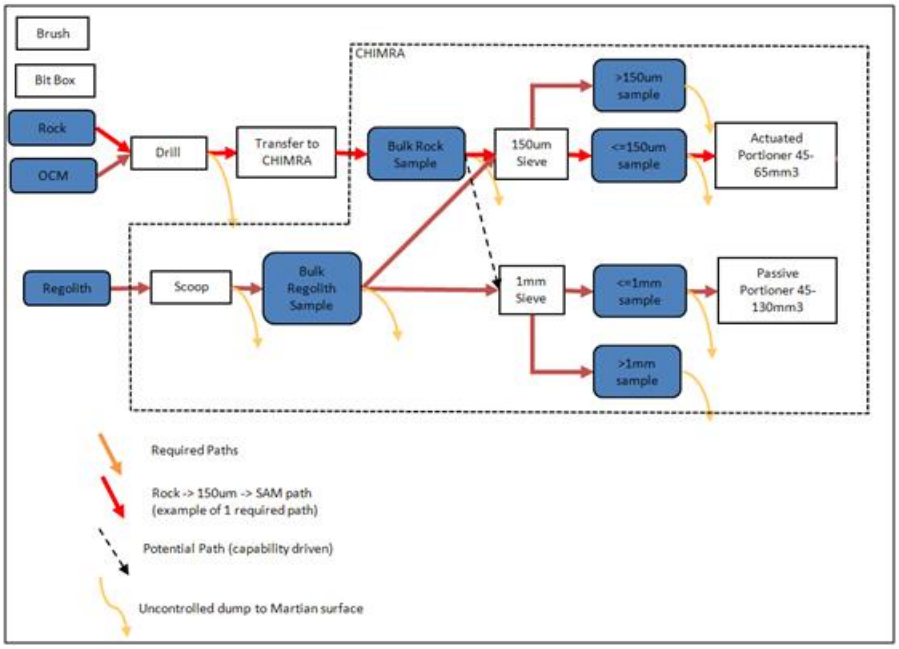

Figure 4. CHIMRA Sample Processing Paths

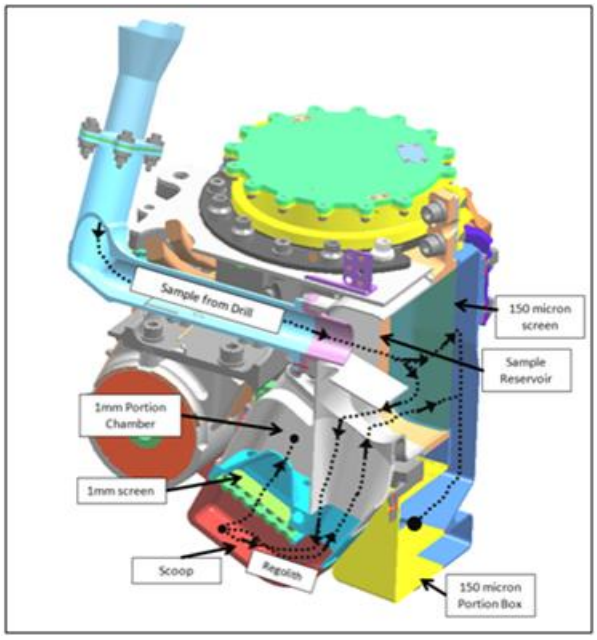

Figure 5. Internal CHIMRA Labyrinths

Figure 6. One-way valves to control flow

In order to create sample flow within its internal passageways, the CHIMRA is vibrated as a whole with a dynamic level of 4-10 G's while it is reoriented with respect to gravity by the Robotic Arm. The dynamic environment is generated by a mechanism that couples the speed of a spinning eccentric mass with the natural frequency of the structure supporting CHIMRA from the turret. This allows the 8-kg CHIMRA to be shaken with a relatively small input force of 150 N. Internal geometric one-way valves (Figure 6) and chamber sizing is used to prevent migration of sample within CHIMRA into unwanted compartments. A combination of dilution cleaning, using chemically understood sample to flush CHIMRA, and forced ejection of clogged particles is used to internally clean CHIMRA between sample processing tasks. Both the 150-micron and 1-millimeter sieves are attached to thwacker mechanisms: a mousetrap mechanism that slams the sieve and frame against a hardstop in order to induce a dynamic impact pulse that ejects clogged particles from the sieve and jolts other internal clogs free.

CHIMRA is composed of four distinct mechanisms, each driven by an actuator: the primary thwack mechanism (PTM), the secondary thwack mechanism (STM), the portion actuator, and the vibration mechanism. Each of the thwack mechanisms performs multiple functions, making configuration of CHIMRA in the required volume achievable by minimizing the number of required actuators. Each actuator in CHIMRA was configured to be supported by a central core structure. This is in contrast to the style of a robotic arm configuration where actuators are supported serially off one another. With a central core configuration, each actuator is only required to move the structure associated with its function. This reduces the output gearbox requirements of a given actuator, lowering the mass and volume required of that device.

The method of creating a sample portion had to both accurately generate a small volume of sample and be robust to the presence of sub-millimeter particle dust. To remove any possibility of an active portion mechanism becoming mechanically clogged or jammed, a passive method of portioning was implemented. Both the 150-micron and 1-millimeter portion chambers contain an open-ended cylinder, or sample tube, that is sized to fill with a specific volume when material is vibrated into it. After bulk sample is brought to the portioning chambers, dynamic excitation and specific rotation of CHIMRA allows gravitational forces to help fill the sample tube, remove excess sample above the tube and eject the sample contained in the cylinder from CHIMRA. The internal geometry that facilitates these actions in the 150 micron portion chamber is illustrated in Figure 7. Once the sample tube is filled, additional vibration levels off the tube and motivates the excess sample to an overflow chamber. The correct portion size is now held in the portion tube while the excess sample is prevented from exiting CHIMRA with the delivered portion. The portion actuator then opens a door at the base of the sample tube and vibration motivates the sample to fall out. After the existing portion is delivered, a new portion can be created by using a 360-degree rotation of the turret to bring the sample in the overflow chamber back above the portion tube. The inclusion of a dedicated portion actuator helps guarantee the ejected sample is less than 150 micron. This is because prior to exiting the sample tube, particles must first pass through the 150-micron screen. A detailed study was conducted on the optimal portion tube geometry to ensure that a consistent portion size is reliably generated and a favorable particle-to-tube-diameter aspect ratio is maintained, thereby minimizing the likelihood of internal arching or tube clogging. The passive method employed by CHIMRA for generating a 150-micron portion provides a consistent portion size without requiring mechanical components that would likely jam when manipulating fine dust particles.

A combination of geometry and internal features allowed a second portioning mechanism to be seamlessly integrated into existing CHIMRA features; this novel configuration removes the need for an additional actuator but sacrifices some portion size consistency. Figure 8 illustrates the features of the scoop and 1-millimeter thwack arm that allow for portion generation. Bulk sample is first sorted by both a four millimeter grate and a 1-millimeter sieve before it is passed through a one-way valve into the 1 millimeter portioning chamber. The purpose of the four millimeter grate is not to sort the sample, but instead to provide structural protection for the fragile 0.05-mm thick, 1-millimeter sieve, in order to ensure that it is not punctured when the scoop is full and closed.

The key element of the STM that allows for portioning functionality is the float between the motion of the secondary thwack arm and the scoop. The secondary thwacker arm is preloaded closed against the scoop. When the scoop is opened the secondary thwack arm will follow the scoop for ten degrees until the STM latch is engaged and the thwack arm restrained. This provides the opportunity to discard all excess sample in the 1-millimeter chamber as well as sample greater than 1 millimeter contained in the scoop. The only sample retained will be what is contained in the portion tube integral to the thwack arm. A bypass valve allows this generated portion to be brought back into the scoop chamber where it can be distributed to the instruments by pouring it out the opened scoop. The sacrifice made by not dedicating an actuator to 1-millimeter portioning is that the generated portion size has the possibility of containing particles that did not pass through the 1-mm screen. Specifically, this is any sample that did not fall out of the scoop at the previous step. This is because the sample distributed to the instruments does not exit CHIMRA from a chamber that can only be accessed by first passing through a screen as is the case with the 150-micron portion design. This shortcoming is mitigated by including a visual inspection step in which the scoop is opened and the sample is visually examined prior to delivery.

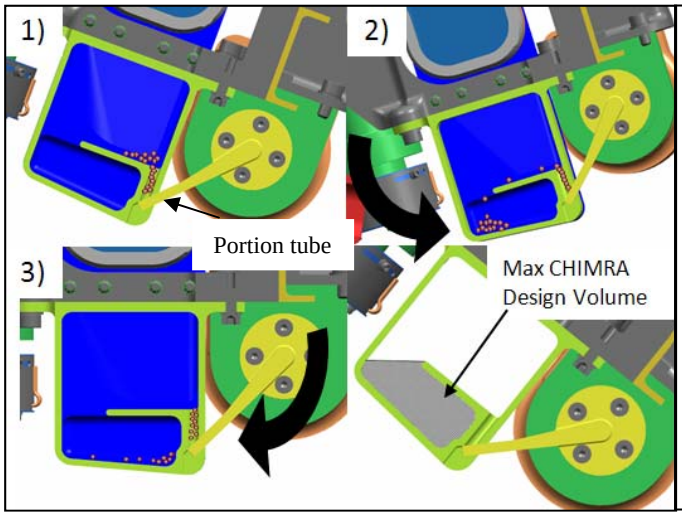

Figure 7. 150-micron Portioning Method

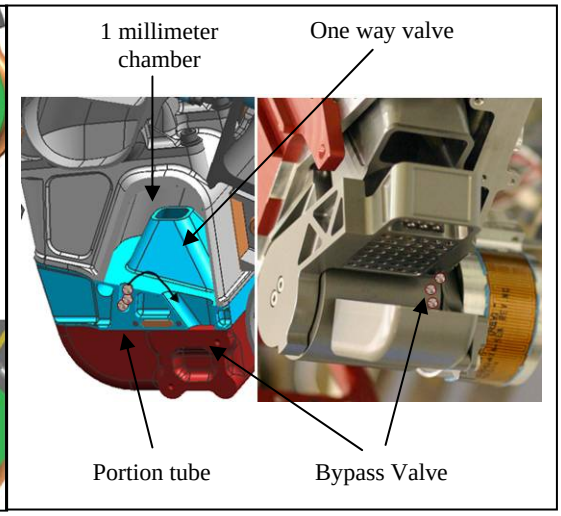

Figure 8. 1-millimeter Portioning Method

Sample Processing Robustness via Design Configuration

With few examples of design heritage to learn from and base the CHIMRA design on, a set of sample handling guidelines was established prior to structuring the CHIMRA layout. This allowed design iterations to be evaluated against predetermined principles that were chosen to maximize the design robustness independent of the implementation constraints. These established guidelines can be broken into two categories: features that minimize the likelihood of internal particle clogging and elements that allow assessment of problems or clogs as they arise. The CHIMRA also required configuration adaptability for sample processing in the case of an actuator failure. These elements established the driving principles behind CHIMRA's sample processing robustness.

While the design features utilized to mitigate clogging are straightforward, the design difficulty for CHIMRA arose when external volume or mass constraints forced compromise between sample processing guidelines and subsystem device requirements. For example, the aspect ratio of a chamber's size to size of a particle passing through that chamber was carefully monitored; the final CHIMRA design strived to maintain a 10:1 aspect ratio. However, this was a compromise from the original 20:1 design philosophy that was eroded as wall thicknesses were increased to meet structural requirements, passageways were reduced to meet subsystem volume allocations, and overall design was changed to

accommodate growing volumes of delivered actuators. Although ultimately reduced, this “order of magnitude” rule of thumb has proven to be successful during development testing of the device. In addition to tracking the aspect ratios of sample passageways, all sample chambers were sized to have at least twice as much internal volume as the maximum sample volume that would be contained, an achievable goal because the sample volume acquired from the drill and the scoop can be controlled and therefore designed around. To avoid unexpected particle behavior in a 3/8 G environment or for a unique rock type, the CHIMRA design intentionally minimizes the frequency of scenarios in which it has to rely on sample to act in a certain manner, such as remaining within one chamber or returning backwards through a screen it had just been sorted through. This latter requirement was stipulated for two reasons: most industry sieves are not symmetric and have a preferred sorting direction and the CHIMRA method of screen unclogging would only unclog sample from a single direction. A common form of clogging found in early testing occurred when an elongated particle would pass though a two-dimensional orifice, change direction and not be able to return through that same entrance. To alleviate this behavior and to ensure that a non-spherical particle does not get trapped within CHIMRA, the exit of any particular chamber was designed to be significantly larger than the entrance. This feature is most notably seen in the exit from the 1-millimeter grate (Figure 9), where a clearing channel was introduced to prevent sample less than 4 millimeter in diameter but greater than 1 millimeter in diameter from becoming stuck between the two screens. Another feature incorporated within CHIMRA was to align the interface between a door and CHIMRA with the rotation axis of the door. This removes the tangential motion between a closing door and CHIMRA which could foreseeably result in a perfectly sized particle creating a Morse taper effect and wedging the door shut.

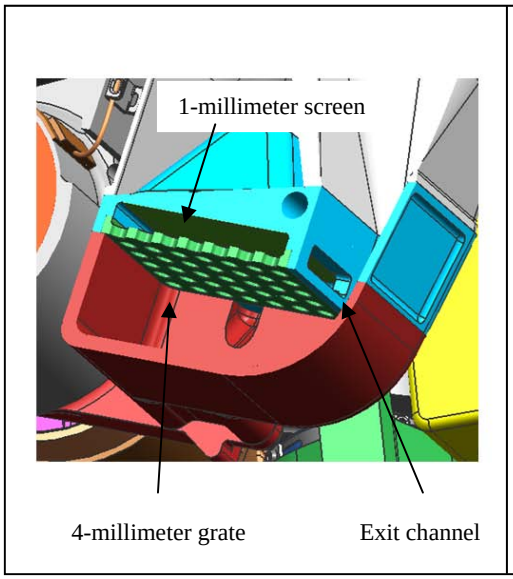

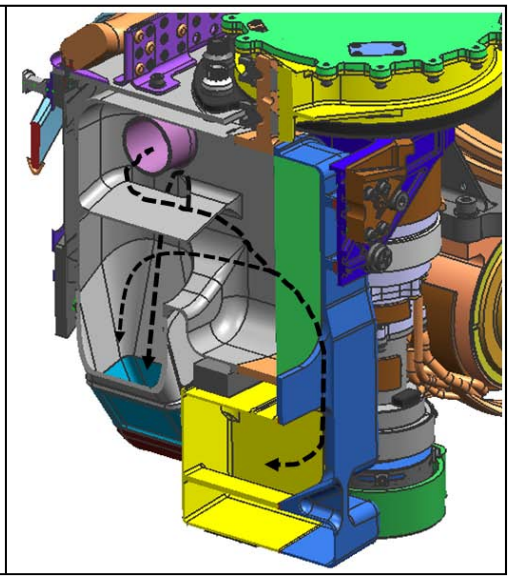

Figure 9. Features to minimize clogging **Figure 10. Sample Diverter Operation**

Of equal importance to anti-clogging features are design elements that allow troubleshooting when performance of the sample processing device begins to degrade. Specifically, the internal layout of CHIMRA allows almost all of the internal surfaces to be visually inspected by an external camera. Additionally, a rover camera can inspect sample prior to delivering portions for instrument ingestion; this provides a checkpoint to give ground operators the option to triage samples that look troublesome for the instruments. CHIMRA minimized the black-box design architecture (sample in/sample out) whenever possible to provide ground operators with maximum opportunity to assess problems as they arise and to adapt operations to prevent repeat incidents. The sample transfer tube that funnels sample from the drill into CHIMRA is the exception to this as it was not possible to include a method of internal visual inspection.

CHIMRA's capacity to adapt to any singular element failure and maintain the ability to process and deliver drilled sample was primarily accomplished through design configuration. If a component of the 150-micron portioning mechanism malfunctions, such as a failed portion actuator or jammed portion tube, the 150-micron sample can be rerouted to the scoop and distributed through the 1-millimeter portioning mechanism. A failure of the scoop or thwack actuator was more problematic to accommodate in design. This is because the internal configuration of CHIMRA that maximizes the internal viewing surfaces results in using both the tunnel and scoop to route sample internally. This meant that an actuator failure in an open configuration could ultimately cause all sample to be lost during processing. To address this, the primary reservoir diverter (Figure 10) was implemented to ensure that sample can still be internally routed to a portioning device without losing the majority of the bulk sample in situations where the tunnel or scoop has failed open. A failed scoop actuator will also not impede sample drop-off to the rover inlets. The relative configuration of the 150-micron portion tube and the scoop swept volume allows CHIMRA to be lowered down to the rover deck to deliver sample even if the scoop actuator is failed open.

It would be naive to assume that CHIMRA potential malfunctions are limited to actuator failures; internal clogging is also a concern. The inclusion of two radically different means of motivating sample within CHIMRA, sinusoidal vibration and high energy impact events, maximizes the likelihood that particles stuck within its cavities can be removed. A notable exception to the self-sufficient redundancy of CHIMRA is a scenario in which the device failure occurs within the vibration mechanism. While the development plan for this scenario was to motivate sample through a portioning chamber by using a thwacking device to vibrate CHIMRA, initial testing suggests that utilizing the drill's percussive voice coil (1) will be more effective in generating internal CHIMRA dynamics.

Although the previously discussed guidelines were already culled from a far greater list that covered implementations more unique to CHIMRA, there are three universal concepts that, above all else, will make CHIMRA a robust and useful tool to the science community for a lifetime on Mars. The first is the ability to view all of the internal areas within CHIMRA to allow ground operators to understand how sample is behaving within CHIMRA and to troubleshoot any problems that arise during mission life. Second, a science sample can be delivered to the rover instruments even in the event of a malfunction. Third, the design configuration allows for multiple methods to motivate sample through CHIMRA. Finally, it is worthwhile to explicitly address the conflict of interest in designing a sample processing stage within a constrained volume. A number of changes can occur during subsystem design maturation: actuator volumes can increase, external volumes can become encroached upon, and structural components or interfaces are increased in size. Each of these changes can be reacted to by shrinking internal passageways; compromising on the features that will ultimately make the device a successful sample processing device. All effort should be made by subsystem configuration engineers to afford the sample processing device a greater volume than is thought to be needed.

Thwack! - Development of the Primary Thwacker Mechanism

The complexity of the PTM and STM does not lie in the mechanism itself as both are essentially simple latch and pawl mechanisms. Instead, the difficulty was in the amalgamation of typical mechanism robustness metrics with the nonstandard and undefined mechanism goals: clearing a screen clogged with an unknown particle type.

Both the PTM (Figure 11) and STM have enough similarities that only the development of the PTM will be discussed in detail. The input to the mechanism is the tunnel base (shown in blue in the cross section). This is the same structure that supports and manipulates the tunnel that facilitates sample movement from the 150 micron screen to the portion box. Contained inside the tunnel base is the latch cartridge and tang assembly. The latch cartridge houses a spring-preloaded Vascomax latch. This latch has redundant rotating surfaces: the latch itself pivots around a pin and the pin is able to rotate independently via the bronze-impregnated, steel-backed bushings that provide the straddling support. The tang assembly is a Vascomax pawl with an internal set of duplexed back-to-back bearings that allow the tang to rotate independently within the tunnel base. The output of the mechanism, shown as yellow in the cross section,

is attached to the 150-micron sieve frame and is supported by a lightly-preloaded, thin-section, back-to-back duplex bearing pair. These two independently rotating elements of the PTM, the tang assembly and mechanism output, are coupled together and attached to a pre-wound spiral spring. In the nominal closed configuration, the thwacker arm is preloaded against CHIMRA. When the tunnel is opened five degrees, the mechanism output and tang assembly are engaged by the latch cartridge fixed inside the tunnel base. Additional rotation of the tunnel base forces the output, sieve frame, and tang assembly to also rotate, lagging five degrees behind the tunnel. This rotation further winds the spring. At the end of the mechanism range of motion, the latch is disengaged from the tang by a non-rotating stop fixed to the static mechanism structure. Once disengaged, the wound spring accelerates the output and sieve frame back into the closed position, generating the inertia impact thwack that is used to eject stuck particles. As the tunnel closes, the latch rides over the backside of the tang, snaps back into the armed state, and resets the mechanism.

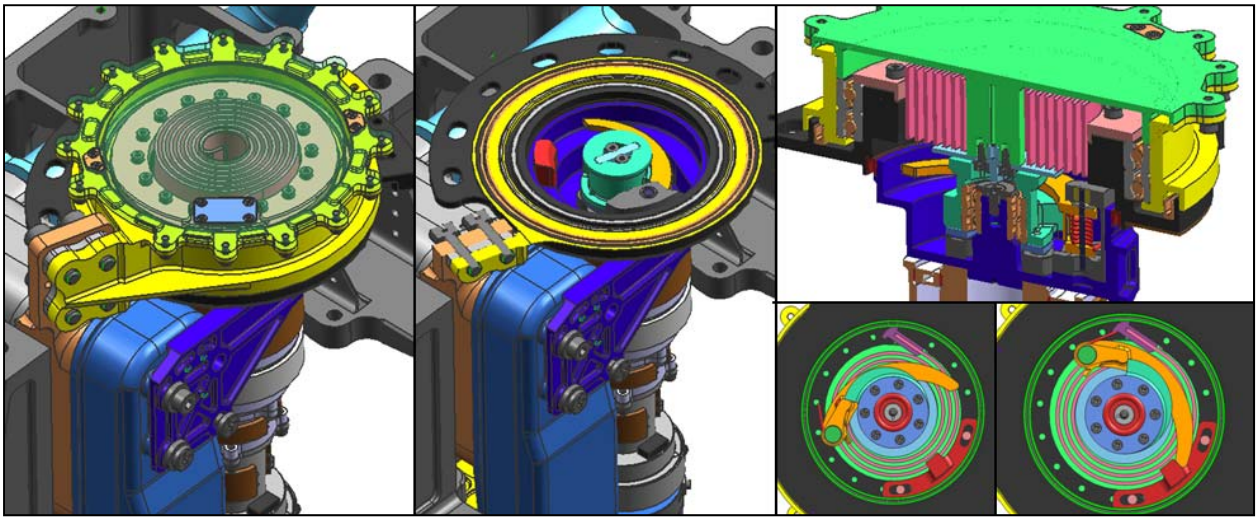

Figure 11. Primary Thwack Mechanism

The primary challenge to overcome in the PTM design was a poor initial test program that resulted in ambiguous functional mechanism requirements. Combining the parameter space of multiple sieve designs, different rock types, and alternating number of thwacks into an efficient development test program meant that only a rudimentary understanding of the phenomena was developed before the design moved on. Additionally, the single life requirement of 500 thwacks made it appear practical to only perform a life test on a single parameter configuration. Therefore, only one full life test was performed early in the CHIMRA life cycle to define the thwack impact speed requirements of the mechanism. This design point was chosen to bludgeon sieve unclogging so that our limited experience was compensated for with a heavily margined impact speed. Early in the CHIMRA design cycle, an impact speed was selected that efficiently unclogged the screen, however left no option to compromise on performance to relax mechanism requirements.

The requirements of the PTM are interconnected in a manner that forced an advanced level of computational design synthesis to meet all functional and traditional mechanism requirements. An inertial dynamic simulator was created in Simulink to allow the spring rate, preload and angular displacement to be modified and simulated. This was used in conjunction with empirical results from targeted cold bearing and seal drag tests to converge upon an acceptable design. While the minimum functional requirements had to be met at the earliest possible thwacker release point, all structural design loads had to account for the last possible release point; this occurs when the spring is at its maximum angular displacement. As the structure was modified to survive these worst case design loads, the rotational inertia of the mechanism increased, forcing the spring energy to increase to maintain the same minimum impact speed. This obviously boosted the impact energy going into the structure and forced additional iterations.

To both maintain the desired thwack impact speed and converge on a structural solution, the range between minimum and maximum release had to be closely controlled.

A computational mechanism simulator was created that modeled the specific mechanism components and forces between them to accurately predict the point of thwack release. Incorporated into this model was a variable range of friction coefficients applied to all sliding surfaces and rotary joints. Because the release angles between the latch and tang depended heavily on the machined final dimensions of the internal mechanism components, a method of inducing variation due to tolerances was incorporated into the mechanism simulator. A standard tolerance stack-up across the mechanism was fed into the simulator to account for how small deviations in part tolerances affected the release point of the mechanism. Finally, the change in mechanism release as a function of component wear at end-of-life was incorporated into the model. The mechanism simulation additionally aided the design because it was able to predict the specific contact angles and surfaces that were frictionally compressed at all moments of the latch release. This allowed internal radii to be dialed in to ensure that local yielding from contact stress did not occur (this was later verified in subcomponent mechanism life test). It was only through this computational design synthesis, which was able to account for frictional dependency, manufacturing tolerances, spring variability and internal component wear, that the range of mechanism release was well understood (Figure 12) and the convergence of a solution that met all functional and traditional requirements of the PTM was possible.

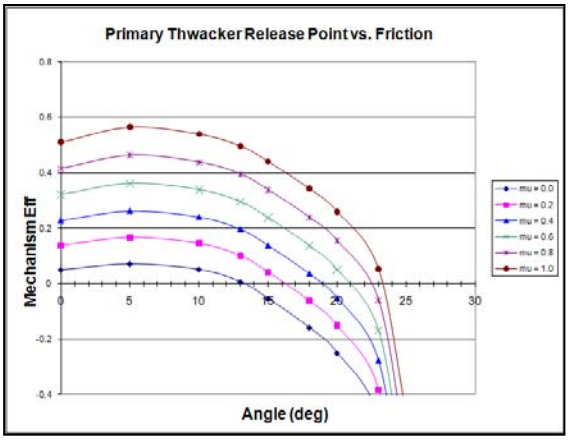

Figure 12. Output of Mechanism Simulator

When assembled and tested, the PTM showed a release point within two-tenths of a degree of where expected and the actual thwack impact speed was predicted within ten percent. During the development and assembly of the PTM, three lessons were learned. 1) Developing a sufficient understanding of the sensitivities in the functional requirements of a mechanism is worth the testing time to find them. This allows changes late in the design phase to be incorporated without re-dialing in the entire mechanism. It was likely that a reduction in the thwack impact speed could have been made and still met unclogging performance metrics, however, the mechanism was unable to capitalize on that possibility due to lack of test data. 2) Mechanisms that have tight requirements on internal alignment should not be split across an interface. As can be seen in the cross section of the mechanism, the upper and lower portions of the mechanism are not explicitly connected. This drove substantial assembly effort to ensure that these two parts were able to be aligned to each other with a high degree of accuracy. 3) The trial-and-error fabrication technique of hand-winding steel springs was not compatible with the high degree of accuracy required for this mechanism. In hindsight, a feature to vary the initial spring preload within the mechanism should have been included. Spring variations had been accounted for in the design by having a settable latch release position, but it would have been far more efficient to modify the initial spring preload when installed in the mechanism.

Good Vibrations: Development of the Vibration Mechanism

The heart and soul of CHIMRA's sample processing ability, the Vibration Mechanism (VM) (Figure 13), is required to generate the dynamic environment CHIMRA uses to flow, sort and portion sample over an operational life of two years and 200 million revolutions. The load generating component of the VM is an eccentric tungsten mass that is supported by two back-to-back, spring-preloaded, angular contact bearings. The motor-side bearing is pressed onto the shaft as well as into the housing; whereas the outboard bearing only contains a press fit on the outer race. The inner race is pressed onto a hollow shaft (green in Figure 13) that slips over the primary shaft of the mechanism. The sliding inner race is then preloaded with a wave spring, reducing the preload sensitivity to assembly tolerances. The central shaft and eccentric mass is driven by the vibration motor through a flexible helical-coupler at speeds between 4000 and 6000 revolutions per minute.

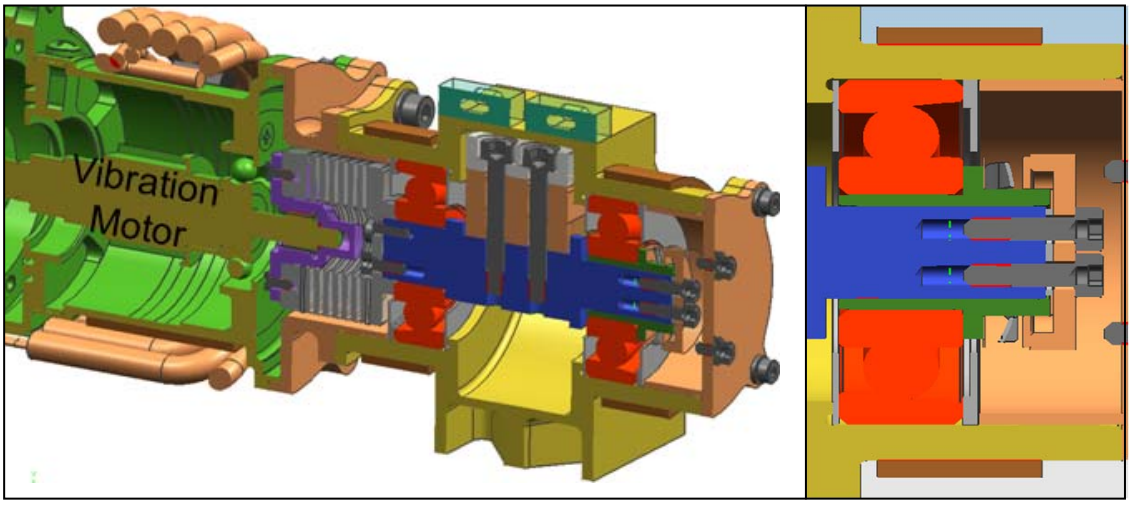

Figure 13. Vibration Mechanism

The torque available from the largest MSL motor was limited when operating at 6000 rotations per minute. This power limitation forced the VM to balance the competing requirements of bearing lubrication drag and long mechanism life. This balance was struck through development testing in the following way. The bearing and lubrication design evolution dictated finding a bearing configuration that produced contact stresses less than 1.38 GPa (200 ksi), converging through test on the maximum lubrication fill factor that afforded acceptable torque margin, and testing the mechanism across the significant life requirements of the device. A development test program was conducted that compared the final lubrication drag across a temperature range of -70 to +70 degrees Celsius for two bearing sizes (10-mm OD and 30-mm OD), two different radial loads (150 and 250 N), three test speeds (4000, 5000 and 6000 rotations per minute) and increasing fill factors working up to 30% fill factor by volume. The bearings were initially greaseplated with Braycote and additional fill factors were generated by inserting a slurry of Braycote grease and Brayco oil. By fabricating and testing three different mechanisms simultaneously, each of the previous variables could be individually varied. When the optimal configuration was found, it was successfully tested past 200 million cycles across a fluctuating temperature profile that represented the flight environment (Figure 14).

A striking result from this testing was that the combination of the parameters unique to this application resulted in visible transitions across three different lubrication regimes: mixed boundary/ elastohydrodynamic , purely elastohydrodynamic and hydrodynamic. For discussion purposes, the 10-mm OD bearing did not display significant changes in performance across the parameter design space and therefore the discussion will focus only on the 30-mm OD bearing. In the vibration mechanism, the load generated from the eccentric mass is proportional to the operating speed squared. However,

testing on both the development unit and the flight unit indicated that the recorded lubrication drag was insensitive to changes in the load applied. This was true even if the load was increased from 100 to 250 N. It is therefore assumed that substantial changes in recorded drag at different operating speeds are primarily a result of the change in speed. Figure 15 illustrates how changes in speed and chamber test temperature affect the lubrication drag within the mechanism. Predicted trends of an inverse relationship between lubrication drag and operating speed were observed. This suggests that increased operating speed is driving the lubrication regime of the bearing from an elastohydrodynamic regime to more hydrodynamic than was expected.

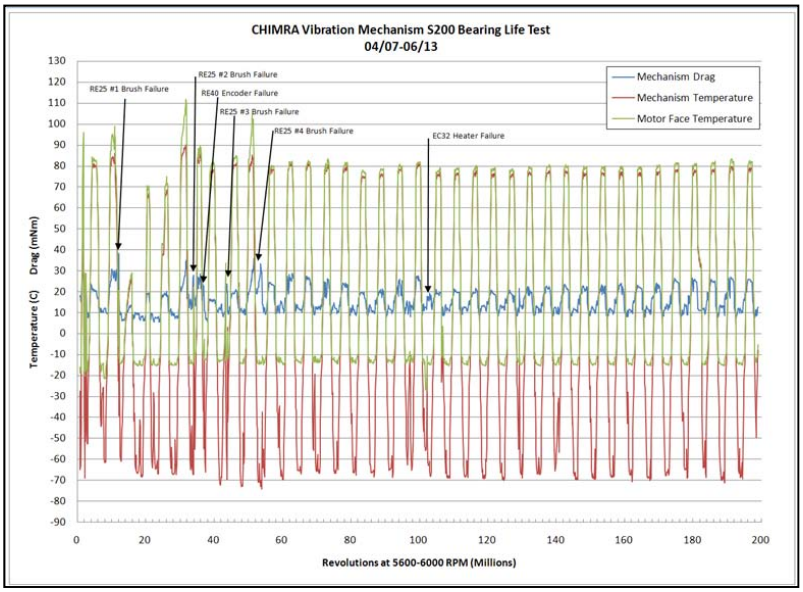

Figure 14. 200-million cycle bearing life test

The transition through different lubrication regimes is also obvious where the expected inverse relation between chamber temperature and lubrication drag was not observed. Specifically, across all three operating speeds, the lubrication drag recorded at -25 degrees Celsius was less than at ambient (20 degrees) and -65 degree Celsius. The low lubrication viscosity at ambient temperatures resulted in a mixed boundary/ elastohydrodynamic operating regime. However, as the temperature decreased to -25 degrees Celsius and viscosity increased accordingly, the regime changed to be pure elastohydrodynamic one and a corresponding lower lubrication drag was recorded. Further decreases in temperature (-65 degrees Celsius) were sufficient to thicken the viscosity to a level where the operating regime of the bearing was hydrodynamic and the corresponding lubrication drag increased beyond that of the elastohydrodynamic regime. This same transition across lubrication regimes was recorded when testing two operating speed across the temperature range on the flight VM (Figure 16) and is consistent with Stribeck Curve Theory (3). A significant increase in drag can be seen when the lubrication fill factor is increased from 15% to 20%. The final parameters selected for the flight configuration were a 30-mm OD bearing with an additional 15% fill factor by volume that is operated at a contact stress of 862 MPa (125 ksi). Once assembled, an infant mortality test was successfully performed that exercised the flight mechanism to 20 million revolutions.

Reflections on Development Testing to Support the Design of a Sample Processing Device

To mature the design of the CHIMRA sample processing system, an extensive suite of development tests were conducted to form a basis of particle flow mechanics. A quick review of the relevant results that the CHIMRA designing principles were based on will provide future designers a more advanced platform to start from when creating a similar design. The results from a series of tests aimed at sample flow across surfaces revealed that both the surface finish and method of surface preparation had a strong effect on

particle retention. All of CHIMRA's sample transfer surfaces are an annealed titanium alloy and hand polished (using a fine grit) to have a smooth surface finish. Both the 150-micron and 1-millimeter screens were 0.05-mm thick and fabricated through a photo-chemical etching process that was compatible with titanium. This temperature compatibility removed a CTE mismatch between the screen and the titanium sieve frame that would result in varying screen tautness across temperature. Sinusoidal vibration was shown to be extremely efficient at motivating particles through chambers similar to CHIMRA as long as the vibration levels were above a floor of 1 G. For the purpose of sorting sample at 150-micron size, it was found that vibration levels of 6 G's or larger in any singular direction motivated sample through the sieve at acceptable rates, however it is important to note that there is an exponential relationship between the sieve throughput by mass and the vibration environment applied. Additionally, having levels around 6G's or greater in two directions motivates sample through a screen substantially better than vibration in only one direction.

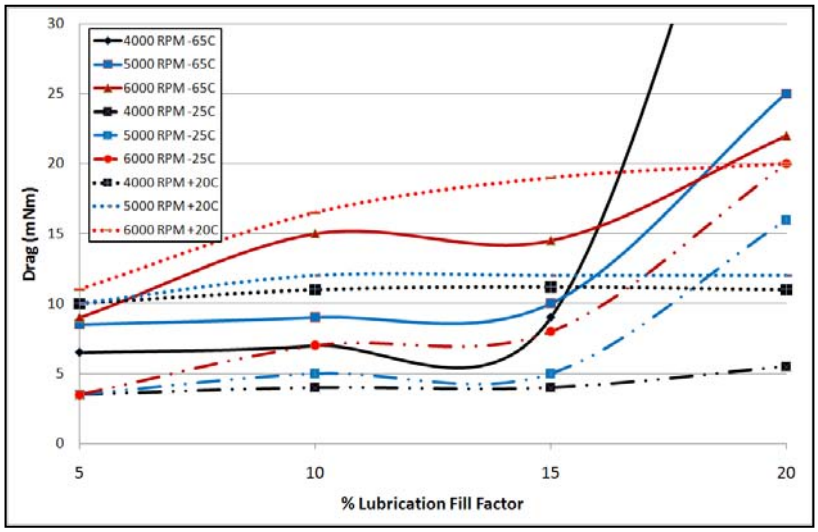

Figure 15. Development Test Unit Drag

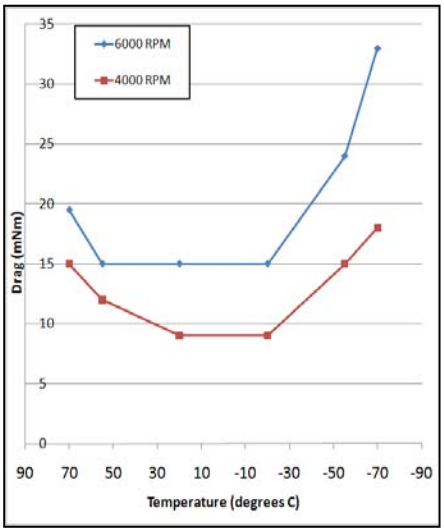

Figure 16. Flight VM Drag

In addition to the specific design points discussed above, global statements from lessons learned during the development testing planning and execution can be made. It is extremely important to conduct all tests where particle interactions between particles or surfaces are being studied in a relevant environment. An important detail to track is the moisture content in the sample and the gas being used to purge the test environment; in fact, because atmospheric moisture can have a drastic effect on the results, test chamber humidity should always be specifically measured and controlled, and sample should be baked out for 24 hours prior to test. A hole in the CHIMRA development test suite that became apparent late in the design was that consecutive runs of alternating relevant samples had never been performed. In fact, these types of tests performed by another instrument on MSL suggest this condition generates the worst electrostatic charge. To allow electrostatic charge to be realistically developed, it is important that all test articles have a similar ground path as the flight unit or be electrostatically isolated to simulate a worst case charge buildup. A final recommendation for similar test programs is to be mindful of how clever a designer gets in attempting to extrapolate results to form conclusions not explicitly tested for. At the time of CHIMRA's design, particle behavior and interactions within a device such as CHIMRA are far from being fully understood and therefore the best way to guarantee a successful design is to explicitly perform tests that mimic the flight application as closely as possible.

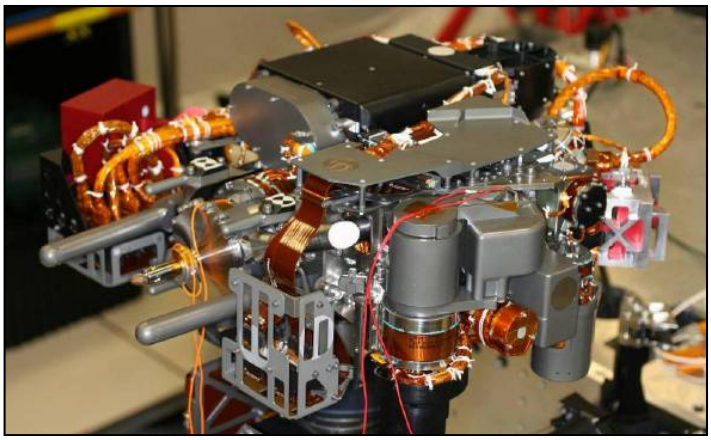

Figure 17. CHIMRA Installed on EM Turret

Conclusions

At the time of writing this paper the qualification and flight CHIMRA mechanisms are being assembled. The engineering model CHIMRA has been functionally tested at ambient conditions and integrated at the next higher level of assembly onto the Robotic Arm as part of the Turret (Figure 17). At this integration level, the dynamics of the CHIMRA when driven by the vibration mechanism were recorded in all relevant robotic arm positions. This test data will be leveraged when the engineering model turret is installed in a pressure chamber on a non-flight robotic arm. In this chamber, the end-to-end sample processing capability of CHIMRA will be tested and verified. It is during this test that the true robustness of CHIMRA as a sampling platform will be measured.

Acknowledgements

The work described in this paper was performed by the Jet Propulsion Laboratory, California Institute of Technology, under contract with the National Aeronautics and Space Administration.

The design, fabrication and assembly of the CHIMRA subsystem would not have been possible without the tremendous amount of dedication, hard work and sacrifice made over a two year period by the CHIMRA team: Andrew Bingham, Dave Berdahl, Cambria Hanson, Joel Johnson, Robert Kovac, Kurt Knutson, Matt Orzewalla and James Wincentsen. A heartfelt thanks goes to those who acted as mentors to myself and my team, providing their own time to ensure the success of CHIMRA: Mark Balzer, Kevin Burke, Randy Foehner, Louise Jandura, Joe Melko, Dave Putnam, Lori Shiraishi, Jeff Umland and Chris Voorhees.

References

1. Okon, Avi. “Mars Science Laboratory Drill.” *Proceedings of the 40th Aerospace Mechanisms Symposium*, (May 2010).
2. Jandura, Louise. “Mars Science Laboratory Sample Acquisition, Sample Processing and Handling: Subsystem Design and Test Challenges.” *Proceedings of the 40th Aerospace Mechanisms Symposium*, (May 2010).
3. Czichos, H. 1978. *Tribology: A systems approach to the science and technology of friction, lubrication and wear*. Amsterdam: Elsevier Scientific Publishing.